Lab on a Chip

PAPER

View Article Online
View Journal | View Issue

Check for updates

Cite this: *Lab Chip*, 2021, **21**, 4805

3D microfluidic cloth-based analytical devices on a single piece of cloth by one-step laser hydrophilicity modification†

Dong Wu, [a] Yinlong Ding,[a] Yuxuan Zhang,[a] Deng Pan,[a] Jiawen Li, *[a] Yanlei Hu, [a] Bing Xu *[b] and Jiaru Chu[a]

Received 19th July 2021,
Accepted 25th October 2021

DOI: 10.1039/d1lc00639h

rsc.li/loc

In this work, we report for the first time a simple and robust method for constructing a 3D microfluidic analytical device on a single piece of hydrophobic cotton cloth. Specifically, laser scanning technology was applied to process hydrophilic regions at the top and bottom of a single piece of hydrophobic cloth. Symmetrical hydrophilic regions at the bottom and top constituted vertical microfluidic channels, and asymmetrical hydrophilic regions constituted transverse flow channels. Liquid flow velocity in 3D cloth-based microchannels can be adjusted flexibly by modifying laser parameters, and programmable laser scanning can be utilized to process 3D microfluidic devices with various patterns. Single-piece 3D cloth-based microfluidic devices formed *via* this method can be used in many fields such as information encryption and anti-counterfeiting, multi-liquid printing and liquid mixing dilution. Compared to traditional processing methods of 3D cloth-based microfluidic devices, the laser scanning method eliminates multiple complex and repetitive assembly processes, which is a significant advance in this research area. This processing method provides a new option for fast and large-scale manufacturing of 3D cloth-based microfluidic analysis devices for point-of-care testing application in undeveloped regions/countries.

Introduction

Point-of-care testing (POCT) is critical for measuring and analyzing the quantity of analytes in resource-limited settings that lack access to laboratory instruments, skilled professionals or electrical power supply.[1] It allows patients or medical staff to accurately obtain real-time, high-quality diagnostic results within minutes.[2] POCT offers benefits of improving efficiency and productivity, simplifying the operating process and procedures, and requiring no complex equipment. A point-of-care analysis device needs to be inexpensive, user-friendly, rapid, equipment-free and deliverable to end-users.[3] Thus, it is highly desirable to develop new techniques and novel materials to manufacture these devices for testing and analyzing in resource-poor areas.

Recently, microfluidic technology has attracted considerable attention for wide applications in POCT cases because it provide a simple way for portable, cheap, disposable and rapid assays and has minimal equipment requirements.[4–6] Initially, due to the low cost, wide availability, disposability, and natural hydrophilicity of paper, microfluidic paper-based analytical devices (μPADs) were proposed by the Whitesides group *via* patterning paper into selectively hydrophilic and hydrophobic patterns.[7] Later, with great effort to search new materials for POCT devices, microfluidic cloth-based analytical devices (μCADs) have been investigated for performing chemical assays.[8] More importantly, μCADs provide a wearable flexible diagnostic platform for real-time testing of human health conditions,[9] such as sweat sensing.[10,11] Most μPADs and μCADs are based on a two-dimensional (2D) configuration, which are fabricated to guide the fluid and analytes to move in the *x*–*y* plane. 3D μPADs or μCADs were proposed to improve the performance of conventional 2D analytical devices.[12–14] Compared to 2D μPADs or μCADs, 3D μPADs or μCADs can effectively control the fluid flow in the vertical and horizontal directions *via* insetting complex 3D structures inside the chips, which can create a more compact microfluidic chip and minimize the quantity of analytes and samples. Additionally, 3D devices can shorten the moving distance in the *z* direction, decrease the operation time of testing and further increase the analysis throughput.[14,15]

So far, a variety of fabrication methods have been proposed to build the fascinating 3D analytical microfluidic devices on

[a] *CAS Key Laboratory of Mechanical Behavior and Design of Materials, Department of Precision Machinery and Precision Instrumentation, University of Science and Technology of China, Hefei 230026, China. E-mail: jwl@ustc.edu.cn*

[b] *School of Mechanical Engineering, Suzhou University of Science and Technology, Suzhou 215009, China. E-mail: xb022@ustc.edu.cn*

† Electronic supplementary information (ESI) available. See DOI: 10.1039/d1lc00639h

paper or cloth, including the use of double-sided sticky tape,[16,17] origami[8,13,18] and spray adhesive glue.[15] For almost all of these methods, 3D micro-analytical devices need to be fabricated by sequential assembly of single layers of 2D microdevices. Thus, they all require multi-step complicated fabrication processes to create individual 2D devices with precise stacking and alignment. Additionally, to form the vertical flow in the *z* direction, it is required to punch holes in the sheets and introduce hydrophilic materials (*e.g.*, cellulose powder and paper debris) into the pores to connect the two contact layers. Another method for creating 3D analytical devices is origami which relies on an external pressure force through a clamp to hold the folded paper/cloth together and achieve precise alignment. However, the resulting microdevices will fail when the pressure is absent or unreliable.

To circumvent the above problems, a new concept of forming 3D microfluidic analytical devices on a single sheet of paper was proposed. Jeong *et al.* demonstrated a simple method to fabricate a 3D μPAD on a single sheet of paper by using conventional double-sided wax printing and heat lamination.[12] The symmetrical wax patterns formed interpenetrating lateral (*x*–*y* direction) and vertical (*z* direction) microchannels which formed a 3D microfluidic network, eliminating complicated alignment, assembly and punching processes. He *et al.* utilized a laser direct-writing technique to control the depth of polymerized photoresist in a paper substrate, resulting in a 3D micro-flow path.[19] In 2018, Park *et al.* created a 3D μPAD *via* double-sided 3D printing on a single sheet of paper.[20] Through double-sided printing of liquid resin and the following photopolymerization, a sample reservoir, multi-detection zones and several microchannels were constructed. As a result, a 3D micro-flow path or a 3D μPAD was successfully obtained. A unique photolithographic method for creating 3D paper-based microdevices on a single sheet of paper was described by Mora *et al.*[21] In their work, a 3D six-level diluter was designed, fabricated and tested, which showed a compact microdevice with a capacity of low sample requirement and rapid mixing and dilution. The above studies demonstrated a promising way to create 3D micro-analytical devices in a single-sheet of paper. Similar to paper, cotton fabric is also a simple and low-cost material to build disposable microfluidic devices,[8,22,23] but fabricating 3D microfluidic devices on a single piece of cloth has not been studied so far. The main reason may be that unlike paper, cotton fabrics generally consist of warp and weft threads, and there are uneven gaps and holes between the warp and weft threads, so it is still a huge challenge to fabricate 3D micro-analytical devices on a single-piece of cloth/fabric.

Here, we presented a simple, rapid and effective method to fabricate 3D μCADs on a single piece of cloth (3D-μCADs@PC) by using a one-step laser-induced double-sided hydrophilicity modification. Specifically, laser-induced hydrophilicity modification meant that laser ablation removed the wax on the surface of natural hydrophobic cotton fibers and exposed the hydrophilic fibers, thus constructing the hydrophilic fiber region. The method can not only flexibly construct various hydrophilic patterns on a hydrophobic cotton cloth to create various three-dimensional microfluidic devices on a single-piece of cloth, but also realize controllable adjustment of liquid velocity by adjusting laser parameters, which is a significant advantage of this method. Finally, we preliminarily explored the functional applications of laser-processed 3D-μCADs@PC in the fields of information encryption, multi-liquid distribution/printing, and liquid mixing/diluting. This work provided a novel method for the construction of simple and low-cost 3D cloth-based microfluidic analysis devices.

Experimental

Materials

The cotton fabric (100% cotton, ~500 μm in thickness, with 32 warp threads per inch and 30 weft threads per inch) used in the experiments was purchased from Hubei Gaojie Textile Co., Ltd (Xiangyang, Hubei). Chemical fiber, polyester, linen and nylon fabrics were purchased from Shandong Yongsheng Textile Co (Linyi, Shandong). The dyes used in the experiments were purchased from Bengbu Jingcheng Chemical Co., Ltd., and a colored solution was obtained by dissolving the dyes in deionized water. The hydrophobic reagent for hydrophobic treatment was Glaco solution (Glaco Mirror Coat Zero, Soft 99 Ltd, Japan). After obtaining informed consent, whole blood samples were taken from healthy donors at the First Affiliated Hospital of the University of Science and Technology of China (Hefei, China). All experiments were conducted according to hospital guidelines ("Human Research Ethics Guide") and approved by the Institutional Ethical Committee (IEC) of the hospital (2021-RE-012). All experiments were performed in compliance with Chinese laws. All blood samples were stabilized with anticoagulant additives, stored in Vacutainer test tubes containing heparin, citrate, and EDTA at 4 °C and used within 7 days of collection. The blood typing reagents were received from Beijing Solarbio Science & Technology Co., Ltd (Beijing, China). The reagents contained monoclonal anti-A, anti-B, and anti-D IgM antibodies (A9020), colorful dyes and buffer. Anti-A and anti-B were a transparent cyan and a transparent yellow solution, respectively, whereas anti-D was a colorless solution.

Laser processing

The hydrophilic area on a hydrophobic cotton cloth was fabricated by raster scanning of femtosecond laser. The laser beam (104 fs, 1 kHz, 800 nm) from a regenerative amplified Ti:sapphire femtosecond laser system (Legend Elite-1K-HE, Coherent) was employed for ablation. During the fabrication process, the laser beam was guided onto the sample *via* a galvanometric scanning system (SCANLAB), which made the laser beam focus and scan along the *x* or *y* coordinate direction. 3D-μCADs@PC were realized by laser scanning hydrophilic patterns on the bottom and top surfaces of a

cotton fabric (Fig. S1†). It takes about two minutes for the laser to process a hydrophilic area of one square centimeter (10 mm × 10 mm).

Hydrophilic depth measurement

We introduced green dye solution to the processing area, cut the cotton fabric after the green dye solution dried, and recorded the depth of colored dye *via* a CCD camera so as to define the depth of the hydrophilic layer.

Characterization

The topographies of the original cotton fabric and the cotton fabric processed by laser were characterized by using a secondary electron SEM (ZEISS EVO18). The contact angles of the water droplet (~4 μL) in air were measured using a CA100C contact-angle system (Innuo) with the sessile drop method. Average values were obtained by measuring five drops at different locations on the same surface. All of the contact-angle measurements were conducted at 10% humidity and 20 °C. The optical images were taken using a charge-coupled-device camera.

Concentration analysis

Images of 3D cloth-based diluters were taken using a mobile phone (Realme X7 Pro), and then the images were analyzed by MATLAB software. We first converted the color images into grayscale images, then the gray average values of the six circular hydrophilic areas in the last line of the diluters were calculated, and the recorded gray values were related to the concentration of the analytes.

Blood type analysis

In the blood type analysis experiments, 8 μL of different antibodies (anti-A, -B and -D) were first added to the three hydrophilic inlets, and the antibodies were rapidly distributed in the three hydrophilic microchannels (A, B and D). 10 min later (for dryness of antibodies), 8 μL of blood samples were respectively added to the three inlets; blood type information can be directly observed from the outlets (Fig. S16a†).

Results

Fabrication of 3D-μCAD@PC by one-step laser scanning

Cotton cloth, an inexpensive lightweight and flexible platform, has been studied as a promising material for creating disposable 2D/3D microfluidic analytical devices.[24–26] The traditional methods usually create hydrophobic barriers on hydrophilic cotton cloth to construct microfluidic channels, then folding or origami was utilized to fabricate 3D microfluidic devices.[8,27] In this study, hydrophilic

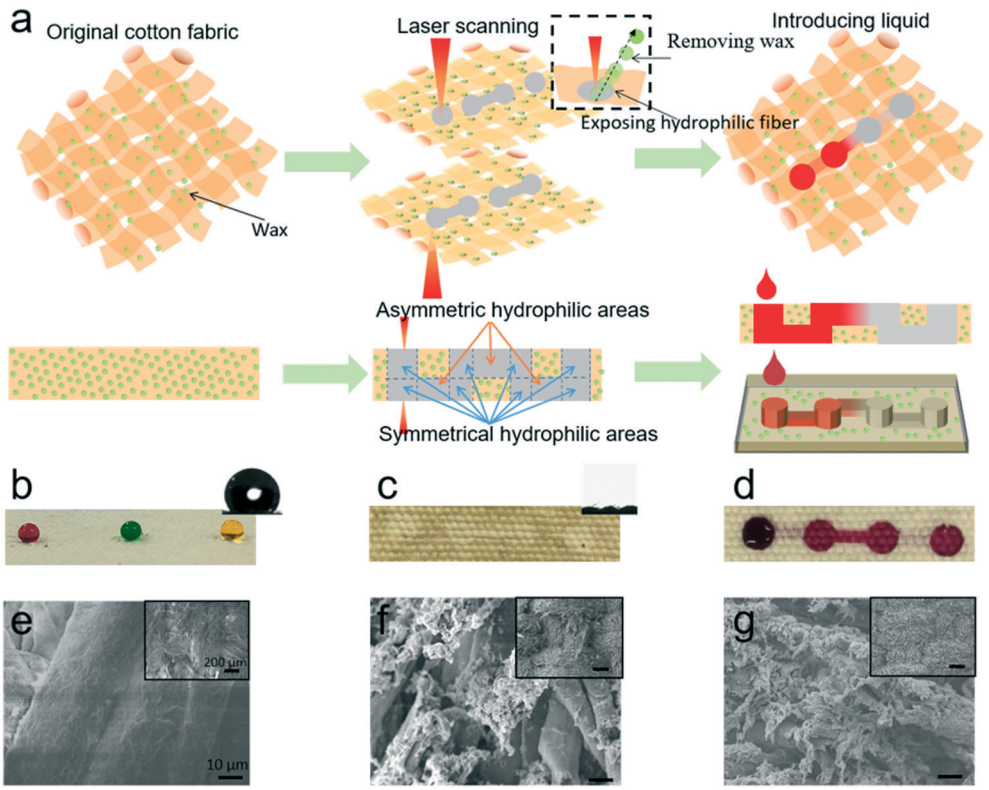

Fig. 1 Fabrication of 3D-μCAD@PC by laser scanning. (a) Schematic diagram of fabrication of 3D-μCAD@PC. (b) Colorful droplets placed on the original cotton cloth; the inset shows the water contact angle. (c) Image of laser-processed cotton fabric and its water contact angle. (d) Flow process of colored drops in the 3D-μCAD. (e–g) SEM images of original cotton fabric, cotton fabric processed by laser with a power of 100 mW, and cotton fabric processed by laser with a power of 200 mW, respectively.

microchannels were created on natural hydrophobic cotton cloths through one-step laser scanning, and 3D-μCADs@PC can be constructed by scanning asymmetric and symmetric hydrophilic regions on the top and bottom surfaces (Fig. 1a). The thickness of the cotton fabrics used in the experiments was 500 μm, which can well display 3D microchannels and be used to study processing parameters.

Due to the presence of natural wax on the natural fiber surface (Fig. 1e), the cotton fabric presented hydrophobicity. The water contact angle on the original fabric surface was 120° ± 3° (Fig. 1b). The fabrication process is shown in Fig. 1a. The wax on the cotton fiber surface was first removed and the surface roughness of the fibers was enhanced through laser ablation (Fig. 1f and g), resulting in a superhydrophilic area (Fig. 1c inset). However, the unprocessed area remained hydrophobic, thus preventing liquid diffusion into the surrounding area (Fig. 1d). After laser processing, the color of the fabric changed from yellow to slightly white (Fig. 1c), which can be easily clarified by the naked eye. Moreover, parameter study showed that the best resolution of the laser processed hydrophilic area was ~100 μm (Fig. S2†). It is worth noting that the superhydrophilicity of the fabricated area was long-term effective (Fig. S3†). The vertical symmetrical areas had enough depth of hydrophilicity, so the upper and lower hydrophilic areas can be connected to form a vertical microchannel. However, the asymmetric hydrophilic area was distributed only on one side of the cloth, which constituted a transverse microchannel (Fig. 1a). Finally, these symmetrical and asymmetrical hydrophilic areas created on a single piece of hydrophobic cotton fabric formed a 3D-μCAD to realize the liquid flow in both horizontal and vertical directions (Fig. 1d). It is worth mentioning that laser processing can also process 3D-μCADs on a hydrophilic cotton fabric with hydrophobic treatment (Fig. S4†). Other than cotton fabrics, we also studied the feasibility of using laser to process 3D-μCADs on chemical fiber, polyester, linen and nylon fabrics. The results showed that 3D-μCADs can also be constructed on nylon fabrics in addition to cotton fabrics (Fig. S5†).

Flow velocity investigation

Flow velocity plays an important role in the microfluidic analysis field. Controlling the flow velocity of the fluid in the microchannel enables fast sample delivery, multi-step sample delivery and improved analytical sensitivity in the microfluidic analysis. In this study, the flow velocity of liquid can be adjusted by using laser parameters. We first designed a simple 3D-μCAD@PC (Fig. 2a and S6†) to investigate the influence of laser parameters on the liquid flow speed. The 3D-μCAD@PC (length: 21 mm) consisted of an inlet, an outlet and connected W-shaped microchannels.[12,21] The diameter of the inlet/outlet was 3 mm, and the microchannel width was 1 mm. Liquid flow experiments showed that the microchannels in the vertical direction were stained with dyes, while the microchannels in the transverse direction were stained only on the processed side (Fig. 2b). Fig. S7† shows the cross section of the 3D-μCAD@PC, which

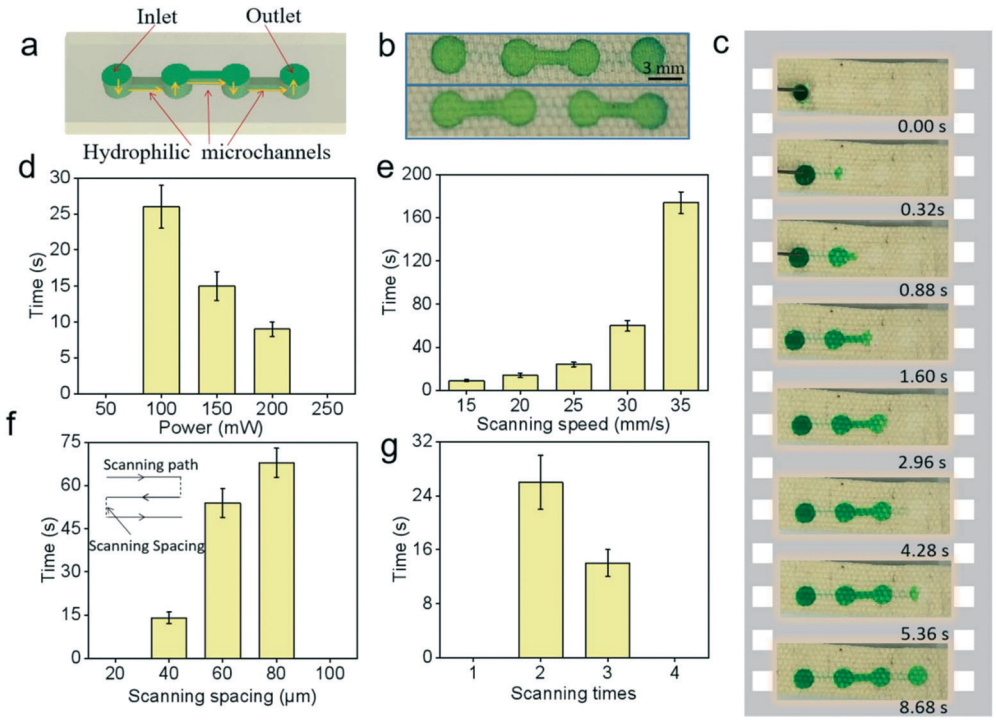

Fig. 2 Flow velocity investigation. (a) Schematic diagram of a 3D-μCAD@PC. (b) Top and bottom views of a 3D-μCAD@PC. (c) Sequence images of the liquid flow process on a 3D-μCAD@PC. (d–g) The influence of laser scanning power, scanning speed, scanning spacing and scanning times on flow velocity.

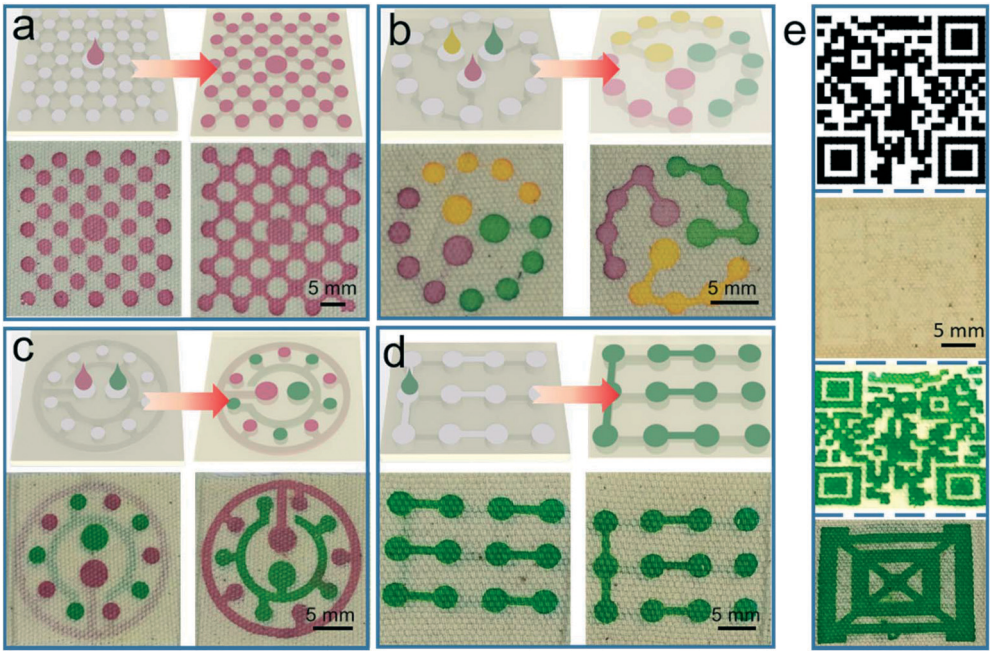

Fig. 3 Laser programmable fabrication of 3D-μCADs. (a–d) Laser processing of various types of 3D-μCADs. Each figure is composed of four small pictures: schematic diagram of the 3D microfluidic channel, schematic diagram of the liquid flow process in the microfluidic channel, top and bottom images of actual 3D-μCADs. (e) Microfluidic device with QR code processed by femtosecond laser. From top to bottom: the QR code, image of laser processing microfluidic device, top view of colored QR code, bottom view of colored QR code.

demonstrates the one-sided hydrophilicity of the microchannel in the transverse direction. ~8 μL of green food dye solution was dropped onto the inlet of the 3D-μCAD@PC to test the flow time. Fig. 3c shows the time-lapsed images of liquid flowing inside the 3D microfluidic channel. When the laser power (*e.g.*, 50 mW) was too low (Fig. 2d), the dye liquid cannot pass through the whole 3D microfluidic channel. Because the laser ablation effect was not obvious, most of the fibers were still covered with hydrophobic wax. With the increasing of laser power, the ablation effect was more significant; thus the hydrophilic cotton fiber can be more exposed. Meanwhile, the roughness of the cotton fibers increased, so the wicking property of the processing area was improved. Once the laser power was too high (*e.g.*, 250 mW), the cotton fibers in the processing area were damaged and became fragile (Fig. S8†). The laser scanning speed was also an important factor (Fig. 2e). Specifically, fast scanning speed can shorten the laser scanning time on the fiber surface, and the wax of the cotton fiber cannot be completely removed. By adjusting the processing speed, the flow velocity can be controlled over a wide range. Liquid can completely pass through the tested 3D microfluidic channel in less than 10 s (*e.g.*, 15 mm s^{-1}) (Video S1†), and the maximum time was ~170 s (*e.g.*, 35 mm s^{-1}) (Video S2†). In addition, the laser scanning spacing was also a factor affecting the flow rate (Fig. 2f). When the scanning spacing was large (*e.g.*, 80 μm), the liquid flow speed was slow due to the presence of a lot of hydrophobic wax in the processed hydrophilic area. Therefore, laser scanning needed to adopt a smaller processing spacing to reduce the hydrophobic wax, thus obtaining a faster wicking speed in the hydrophilic area. Finally, in order to fully remove wax from a thick cotton cloth, it is better to repeat the processing of cotton fabric. In the case of shorter processing times, the dye liquid cannot pass through the whole 3D microfluidic channel (*e.g.*, 1 time). Increasing the processing times can speed up the flow rate, while too many times of scanning will destroy the integrity of the cotton fabric (*e.g.*, 4 times) (Fig. 2g). In addition, we also studied the influence of laser scanning power on the thickness of the hydrophilic layer. We processed the hydrophobic cotton fabric with a laser power of 100 mW, 150 mW, 200 mW, and 250 mW, then measured the depth of the hydrophilic layer. It can be clearly observed that with the increase of laser scanning power, the processed hydrophilic layer was deeper (Fig. S9†). In conclusion, wicking time and hydrophilicity depth can be flexibly controlled by adjusting the laser scanning parameters.

Fabrication of a variety of 3D-μCADs@PC

Laser scanning technology can not only control liquid flow velocity but also provide convenience for programmable fabrication of hydrophilic patterns. We took advantage of the programmable ability of laser scanning to fabricate a variety of 3D-μCADs@PC (Fig. 3a–d). In Fig. 3a, red dye solution was added to the central area of the 3D-μCAD@PC. As the liquid flowed, each circular hydrophilic area was connected by bottom microchannels to form a liquid array (Video S3†). As shown in Fig. 3b and c, different color dye solutions were added to several

slightly larger circular hydrophilic areas to realize the distribution of liquid in different areas. Green dye solution was added to the inlet of the 3D-μCAD@PC (Fig. 3d) and the liquid was distributed along three branches. These 3D hydrophilic channels and patterns constructed on hydrophobic cotton fabrics may have potential applications in the field of wearable sweat detection. In addition, we also processed a complex QR code on a single piece of hydrophobic cotton fabric. We first processed the hydrophilic QR code pattern on the top layer of the cotton fabric and then created connected channels at the bottom of the cotton fabric. In this way, we added green dye solution to the microchannel side of the bottom layer, and the top layer displayed the colored QR code pattern (Video S4†) which can be quickly identified by scanning with a mobile phone (Fig. 3e).

The applications of 3D-μCADs@PC in information encryption/multi-liquid printing

In our experiments, we found that the visibility of the laser-processed patterns was variable with different scanning spacing. Specifically, a large scanning spacing would induce an unclear processed area. The character of laser-processed cotton fabric has potential applications in the fields of anti-counterfeiting and information encryption. Here, we showed a simple encryption microchip on a piece of cloth. The chip contained an inlet and channel regions in the bottom and encryption area, of which the two front areas utilized small scanning intervals (40 μm) and the third area employed large scanning spacing (120 μm). Due to the obvious visibility of the processing pattern, we can simply add colored droplets in the inlet, while the processing trace of the encryption area was not obvious (Fig. 4a and b), which hid the relevant information. One can drip the colorful liquid into the visible inlet, then the liquid flows through the bottom hydrophilic channel and reaches the encryption area; finally the encryption area displays the hidden information through color rendering (Fig. 4b and Video S5†). Another application is the distribution of a variety of liquids and multiple colorful liquid printing *via* laser-processed chips, where the front and back sides of the chips were microchannels and arrays of hydrophilic zones (Fig. S10†), respectively. Dropping colored liquid on the side of the microchannels enabled the liquid to be distributed in 36 hydrophilic zones, thus forming a liquid array. Fig. 4c and d show two different kinds of liquid arrays realized by processing channels of different shapes (Fig. S10†). The shapes of liquid arrays can also be adjusted flexibly *via* programmable laser scanning (Fig. 4e and f). The 3D microfluidic liquid arrays can be used as a stamp (Fig. S11†), which can be utilized to print different colored dye solutions in a variety of shapes and patterns (Fig. 4c–f). Also, the printing results had fine uniformity and integrity.

Diluters on a single piece of cotton cloth

Finally, similar to that of Mora's work,[21] a six-level diluter with the same function was constructed on a single piece of

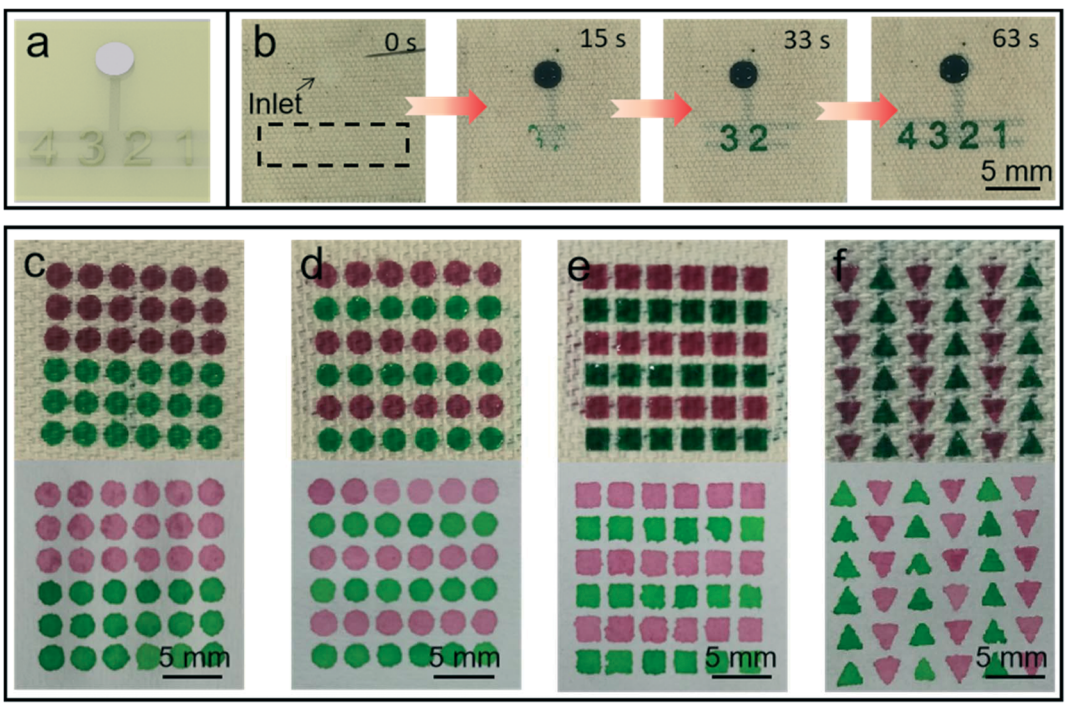

Fig. 4 The applications of 3D-μCADs@PC in information encryption and multi-liquid distribution/printing. (a) Schematic diagram of 3D-μCAD for information encryption. The processing trace in the inlet was obvious, while that in the information encryption area was not obvious. (b) Sequence images of displaying encryption information. (c–f) 3D-μCADs were used for liquid distribution and multiple solution printing.

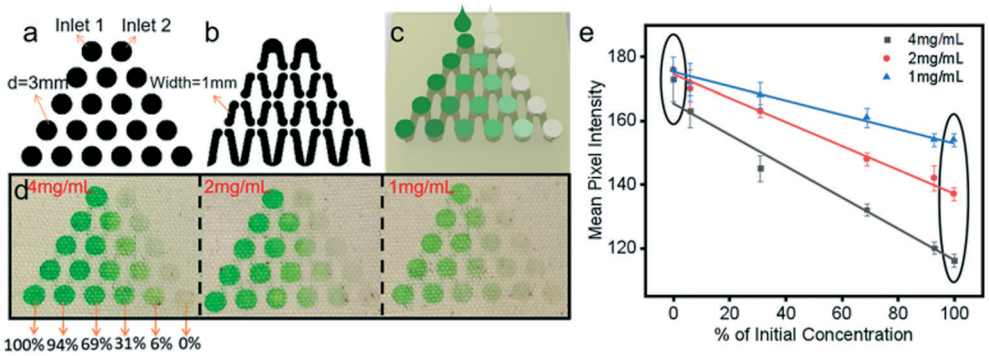

Fig. 5 Diluter processing by laser on a single piece of hydrophobic cotton cloth. (a) Top: pattern of six-level diluter. (b) Bottom: channel pattern of six-level diluter. (c) 3D schematic diagram of diluter. (d) Images of dilution results of 4 mg mL^{-1}, 2 mg mL^{-1} and 1 mg mL^{-1} green food dye solution. (e) Plot of the color intensity in each circle after performing dilutions of 4, 2, and 1 mg mL^{-1} of green dye solution with water. Each point in the graph corresponds to the average gray value from the grayscale images (n = 3) of each detection area.

cloth *via* the laser scanning technique. The hydrophilic zone in the top layer contained a hydrophilic circular array (diameter: 3 mm) (Fig. 5a). The bottom layer had hydrophilic channels with a width of 1 mm (Fig. 5b and S10†). The overlap between the top layer and the bottom layer created hydrophilic channels in the vertical direction which allowed the liquid to flow from top to bottom and from bottom to top. We added a 25 μL known concentration of dye solution to the left inlet while introducing the same volume of deionized water to the right inlet (Fig. 5c). When the liquid had passed through the six hydrophilic areas situated on the lower side of the device, we recorded the result of the diluter. The expected concentration of the dye at each detection area correlated with the measured color intensity at the outlet. After obtaining the images of each experiment, we calculated the gray value of pixel points in each test area. In theory, the ratio of the concentration at each point from left to right to that of the original solution was 100% (original solution), 93.8%, 68.8%, 31.2%, 6.20%, and 0% (deionized water). In our experiments, we employed the dye solution at three different concentrations (Fig. 5d). For each initial concentration, we performed 3 repeat experiments and then plotted the relationship between the color intensity of each test area and the percentage of the initial concentration in each test area (Fig. 5e). As can be seen from Fig. 5e, when the percentage of the initial concentration was 0%, the three curves converged to a common value (~174). This was because 0% initial concentration corresponds to pure water (as previously mentioned). Fig. 5e also shows that the gray values corresponding to 100% original solution were greatly different. The higher the dye concentration was, the lower the gray value was (corresponding to the darker area in the gray image). In addition, it can be observed from Fig. 5e that there was a linear relationship between the solution concentration and the pixel gray value. Finally, we calculated the concentration values at each point in Fig. 5e through the calibration curve of dye solution on a cloth (Fig. S12†). As Fig. S13† shows, the calculated values of concentration at each point in the detection area are well correlated with the theoretical concentration, thus confirming the effective dilution of our 3D-μCADs. Noting that the diluter fabricated in a single piece of cotton fabric here is relatively simple, this strategy can also be extended to manufacturing other devices for more complex applications, such as enzymes or inhibitors, performing titrations and colorimetric analysis.

Discussion

The traditional methods of constructing 3D microfluidic systems mainly involve the deposition of hydrophobic polymers to create hydrophilic microchannels on hydrophilic substrates, and they can be treated as additive methods. In this paper, the method is to transform the hydrophobic region into a hydrophilic region by laser processing on a single piece of hydrophobic cotton fabric, which can be treated as a subtractive method. Usually, hydrophobic wax is present in the whole thickness direction of natural cotton fabric. Laser scanning can remove hydrophobic wax in the partial depth of the z direction and expose hydrophilic fiber; thus, a certain depth of hydrophilic region can be constructed (Fig. S9†). Therefore, it is possible to construct a 3D-μCAD in which two microchannels cross but do not encounter each other in 3D space. Here, we processed two hydrophilic microchannels on the top and bottom surfaces of hydrophobic fabric with a thickness of 2 mm (Fig. S14†). The inlet and outlet areas were processed using high laser power (300 mW), and the microchannel area was processed using low laser power (80 mW). In this way, the liquid in the inlet and outlet areas can flow vertically, while the microchannel area can only flow horizontally. Red and green dye solutions were added to one end of the two channels, respectively. The result demonstrated that the two dye solutions did not intersect. In addition to thick cloths, 3D-μCADs can also be processed on thin cloths (*e.g.*, thickness of 180 μm) through using a lower laser power (50–70 mW) (Fig. S14†). Thus, the above results showed the versatility of laser processing technology on cloths of different thickness.

The fabrication of 3D microfluidic analysis devices on paper materials has been studied extensively for a long time, from the

initial construction by folding and stacking methods to the latest construction methods on single sheets of paper materials. However, the research on the construction of 3D microfluidic devices on cloth materials is still based on multi-layer folding or stacking methods, and the construction of 3D microfluidic devices on a single piece of cotton has not been studied so far. The main reason may be because there is a big difference between cotton and paper. Specifically, paper is made up of many wooden fibers, which are closely connected with each other with the help of a variety of fillers. Cloth is made of many warp and weft threads with large or small gaps between them. Compared to paper, the structure of cotton cloth has greater heterogeneity. Therefore, it is a relatively big challenge to build a functional 3D microfluidic device on a single piece of cloth with a thickness of several hundred micrometers. In this work, 3D microfluidic devices are successfully constructed on a single-piece of hydrophobic cotton cloth for the first time by using laser scanning technology. This technology realizes the robust fabrication of 3D microfluidic analysis devices, reduces the process complexity of 3D microfluidic devices, and promotes the development of 3D-μCADs.

Lastly, we designed blood type analysis devices based on 3D-μCADs. The device enabled rapid and accurate analysis of blood type through RBC agglutination (RBC agglutination reaction can be created *via* blood type A with anti-A, blood type B with anti-B, blood type AB with anti-A/anti-B and blood type RhD+ with anti-D), filtering and blocking the effect of vertical channels on agglutinated RBCs in 3D-μCADs (Fig. S15†).

As Fig. S16d† shows, once the blood was loaded at the inlets, the flow of the blood through the vertical channel allowed the blood and antibodies to fully come in contact and react. If the antibodies preloaded in the channel (*e.g.*, anti-A) were the corresponding antibodies to the antigens carried by the RBCs of the blood sample (*e.g.*, A-type blood), RBC agglutination reaction would first occur in the inlet area. Then, the agglutinated RBCs with large size would be easily filtered by the fibers and cannot reach the outlet (Fig. S16d†). If the antibody in a microchannel was not the corresponding antibody to the antigens carried by the RBCs of the blood sample, RBC agglutination reaction would not occur; thus, non-agglutinated RBCs can easily reach the outlet through the hydrophilic microchannel and displayed red on the outlet area (Fig. S16d†). For example, when blood type A+ was added at the inlets of the device, blood (red color) was eventually observed at outlet B and no blood (no red) was observed at outlets A and D (Fig. S16b†) because blood type A + carried antigen-A and antigen-D but not antigen-B. Tests for other blood types have also yielded reliable results (Fig. S16c†). The study confirmed the feasibility and great potential of developing low-cost, efficient and rapid analytical equipment based on 3D-μCADs.

Conclusion

In summary, we demonstrate the construction of 3D microfluidic analysis devices by laser scanning on a single piece of natural hydrophobic cotton fabric. This technology allows the flexible construction of 3D microfluidic devices with various shapes and enables controlling the flow rate of liquid in the microfluidic channel. We also demonstrate the applications of 3D-μCADs@PC in the fields of droplet printing, information encryption and liquid dilution. Our work has pioneered the construction of 3D microfluidic systems on a single piece of cotton fabric, provided a new avenue for manufacturing point-of-need devices, and demonstrated a new option for performing fast and inexpensive testing in resource-limited areas.

Conflicts of interest

There are no conflicts to declare.

Acknowledgements

This work was supported by the National Natural Science Foundation of China (Grant No. 52105583), the Fundamental Research Funds for the Central Universities (Wk2090000016, WK5290000001) China Postdoctoral Science Foundation (No. 2019M662190), and the Open Project of Wuhan National Laboratory for Optoelectronics (No. 2019WNLOKF014). The authors acknowledge the Experimental Center of Engineering and Materials Sciences at USTC for the fabrication and measuring of samples. This work was partly carried out at the USTC Center for Micro and Nanoscale Research and Fabrication.

References

1 I. Michael, *et al.*, A fidget spinner for the point-of-care diagnosis of urinary tract infection, *Nat. Biomed. Eng.*, 2020, **4**(6), 591–600.
2 M. S. Bhamla, *et al.*, Hand-powered ultralow-cost paper centrifuge, *Nat. Biomed. Eng.*, 2017, **1**(1), 1–7.
3 C.-H. Liu, *et al.*, Blood Plasma Separation Using a Fidget-Spinner, *Anal. Chem.*, 2019, **91**(2), 1247–1253.
4 H. Li, *et al.*, SLIPS-LAB-A bioinspired bioanalysis system for metabolic evaluation of urinary stone disease, *Sci. Adv.*, 2020, **6**(21), eaba8535.
5 C. Liu, *et al.*, A high-efficiency superhydrophobic plasma separator, *Lab Chip*, 2016, **16**(3), 553–560.
6 S. Vemulapati and D. Erickson, HERMES: rapid blood-plasma separation at the point-of-need, *Lab Chip*, 2018, **18**(21), 3285–3292.
7 A. W. Martinez, *et al.*, Patterned paper as a platform for inexpensive, low-volume, portable bioassays, *Angew. Chem., Int. Ed.*, 2007, **46**(8), 1318–1320.
8 A. Nilghaz, *et al.*, Flexible microfluidic cloth-based analytical devices using a low-cost wax patterning technique, *Lab Chip*, 2012, **12**(1), 209–218.
9 X. Liu and P. B. Lillehoj, Embroidered electrochemical sensors for biomolecular detection, *Lab Chip*, 2016, **16**(11), 2093–2098.
10 A. Koh, *et al.*, A soft, wearable microfluidic device for the capture, storage, and colorimetric sensing of sweat, *Sci. Transl. Med.*, 2016, **8**(366), 366ra165.

11 J. T. Reeder, *et al.*, Waterproof, electronics-enabled, epidermal microfluidic devices for sweat collection, biomarker analysis, and thermography in aquatic settings, *Sci. Adv.*, 2019, **5**(1), eaau6356.
12 S.-G. Jeong, *et al.*, Toward instrument-free digital measurements: a three-dimensional microfluidic device fabricated in a single sheet of paper by double-sided printing and lamination, *Lab Chip*, 2015, **15**(4), 1188–1194.
13 H. Liu and R. M. Crooks, Three-Dimensional Paper Microfluidic Devices Assembled Using the Principles of Origami, *J. Am. Chem. Soc.*, 2011, **133**(44), 17564–17566.
14 A. W. Martinez, S. T. Phillips and G. M. Whitesides, Three-dimensional microfluidic devices fabricated in layered paper and tape, *Proc. Natl. Acad. Sci. U. S. A.*, 2008, **105**(50), 19606–19611.
15 G. G. Lewis, *et al.*, High throughput method for prototyping three-dimensional, paper-based microfluidic devices, *Lab Chip*, 2012, **12**(15), 2630–2633.
16 G. G. Lewis, M. J. DiTucci and S. T. Phillips, Quantifying Analytes in Paper-Based Microfluidic Devices Without Using External Electronic Readers, *Angew. Chem., Int. Ed.*, 2012, **51**(51), 12707–12710.
17 A. W. Martinez, *et al.*, Programmable diagnostic devices made from paper and tape, *Lab Chip*, 2010, **10**(19), 2499–2504.
18 L. Ge, *et al.*, 3D Origami-based multifunction-integrated immunodevice: low-cost and multiplexed sandwich chemiluminescence immunoassay on microfluidic paper-based analytical device, *Lab Chip*, 2012, **12**(17), 3150–3158.
19 P. J. W. He, *et al.*, Laser direct-write for fabrication of three-dimensional paper-based devices, *Lab Chip*, 2016, **16**(17), 3296–3303.
20 C. Park, *et al.*, Double-sided 3D printing on paper towards mass production of three-dimensional paper-based microfluidic analytical devices (3D-mu PADs), *Lab Chip*, 2018, **18**(11), 1533–1538.
21 M. F. Mora, *et al.*, Patterning and Modeling Three-Dimensional Microfluidic Devices Fabricated on a Single Sheet of Paper, *Anal. Chem.*, 2019, **91**(13), 8298–8303.
22 P. Bhandari, T. Narahari and D. Dendukuri, 'Fab-Chips': a versatile, fabric-based platform for low-cost, rapid and multiplexed diagnostics, *Lab Chip*, 2011, **11**(15), 2493–2499.
23 M. Liu, *et al.*, Battery-triggered open wireless electrochemiluminescence in a microfluidic cloth-based bipolar device, *Sens. Actuators, B*, 2017, **246**, 327–335.
24 M. Liu, *et al.*, A low-cost, ultraflexible cloth-based microfluidic device for wireless electrochemiluminescence application, *Lab Chip*, 2016, **16**(15), 2860–2870.
25 R. Safavieh, G. Z. Zhou and D. Juncker, Microfluidics made of yarns and knots: from fundamental properties to simple networks and operations, *Lab Chip*, 2011, **11**(15), 2618–2624.
26 P. Wu and C. Zhang, Low-cost, high-throughput fabrication of cloth-based microfluidic devices using a photolithographical patterning technique, *Lab Chip*, 2015, **15**(6), 1598–1608.
27 B. Xu, *et al.*, Cloth-based microfluidic analytical devices by laser-induced hydrophilization technique, *Sens. Actuators, B*, 2021, **341**, 129998.